8

Acoustic and Electroacoustic Spectroscopy for Characterizing Emulsions and Microemulsions

Andrei S. Dukhin and P. J. Goetz
Dispersion Technology Inc., Mount Kisco, New York

T. H. Wines and P. Somasundaran
Columbia University, New York, New York

I. INTRODUCTION

The widespread acceptance and commercialization of acoustic spectroscopy has been slow to develop. This technique has been overlooked by many in academia and industry in the past, but has recently been showing increased levels of accptance. This powerful method of characterizing concentrated heterogeneous systems has all the capabilities for being successful. The first hardware for measuring acoustic properties of liquids was developed more then 50 year ago at the Massachusetts Institute of Technology (1) by Pellam and Galt. The first acoustic theory for heterogeneous systems was created by Sewell 90 years ago (2). The general principles of the acoustic theory were formulated 47 years ago by Epstein and Carhart (3). There is a long list of applications and experiments based on acoustic spectroscopy —see reviews (4, 5). Despite all of these developments, however, acoustic spectroscopy is rarely mentioned in modern handbooks on colloid science (6, 7).

Acoustics is able to provide reliable particle size information for concentrated dispersions without any dilution. There are examples when acoustics yields size information at volume fractions above 40%. This insitu characterization of concentrated systems makes the method very useful and unique in this capability compared to alternative methods, including light scattering, where dilution is required. Acoustics is also able to deal with low dispersed phase volume fractions and in some systems can characterize down to below 0.1% vol. This flexibility for concentration range provides an overlap with classical methods for dilute systems. In the overlap range, acoustics size characterization has been found to have excellent agreement with these other techniques.

Acoustics is not only a particle sizing technique, but also provides information about the microstructure of the dispersed system. The acoustic spectrometer can be considered as a microrheometer. In acoustics, stresses are applied in the same way as with regular rheometers, but over very short distances on the micrometer scale. In this way, the microstructure of the dispersed system can be sensed. Currently, this feature of acoustics is only beginning to be exploited, but it is certainly very promising.

Many people have perceived acoustics to have a high degree of complexity. The operating principles are in fact quite straightforward. The acoustic spectrometer generates sound pulses that pass through a sample system and are then measured by a receiver. The passage through the sample system causes the sound energy to change in intensity and phase. The acoustic instrument measures the sound energy losses (attentuation) and the sound speed. The sound

attenuates due to interaction with the particles and liquid in the sample system. Acoustic spectrometers generally operate in the frequency range 1-100 MHz. This is a much higher sound frequency than the upper limit of our hearing which is only 0.02 MHz.

While the operating principles are relatively simple, the analysis of the attenuation data to obtain particle size distributions does involve a degree of complexity in fitting experimental results to theoretical models based on various acoustic loss mechanisms. The advent of high-speed computers and the refinement of these theoretical models has made the inherent complexity of this analysis of little consequence. In comparison, many other particle sizing techniques such as photoncorrelation spectroscopy also rely on similar levels of complexity in analyzing experimental results.

Acoustics has a related field that is usually referred to as "electroacoustics" (8). Electroacoustics can provide particle size distribution as well as zeta potential. This relatively new technique is more complex than acoustics because an additional electric field is involved. As a result, both hardware and theory become more complicated. There are even two different versions of electroacoustics depending on what field is used as a driving force. Electrokinetic sonic amplitude (ESA) involves the generation of sound energy caused by the driving force of an applied electric field. Colloid vibration current (CVC) is the phenomenon where sound energy is applied to a system and a resultant electric field or current is created by the vibration of the colloid electric double layers.

Returning to acoustics, its lack of widespread acceptance may be related to the fact that it yields too much, sometimes overwhelming, information. Instead of dealing with interpretation of the acoustic spectra it is often easier to dilute the system of interest and apply light-based techniques. It was often naively assumed that the dilution had not affected the dispersion characteristics. Lately, many researchers are coming to the realization that dispersed systems need to be analyzed in their natural concentrated form, and that dilution destroys a number of useful and important properties.

We are optimistic about the future of acoustics in colloid science. It is amazing what this technique can do especially in combination with electroacoustics for characterizing electric surface properties. We hope that this review will allow you to taste the power and opportunities related to these sound-based techniques.

II. THEORETICAL BACKGROUND

There are six known mechanisms for the ultrasound interaction with a dispersed systsem: (1) viscous; (2) thermal; (3) scattering; (4) intrinsic; (5) structural; and (6) electrokinetic. Here, we give only short qualititive descriptions, omitting complicated mathematical models.

1. The viscous losses of the acoustic energy occur due to the shear waves generated by the particle oscillating at the acoustic pressure field. These shear waves appear because of the difference in the densities of the particles and medium. This density contrast causes particle motion with respect to the medium. As a result, the liquid layers in the particle vicinity slide relative to each other. This sliding nonstationary motion of the liquid near the particle is referred to as the "shear wave". Viscous losses are dominant for small rigid particles with sizes below 3 μm, such as oxides, pigments, paints, ceramics, cement, graphite, etc.
2. The reason for the thermal losses is the temperature gradients generated near the particle surface. These gradients are a result of the ther modynamic coupling between pressure and temperature. This mechanism is dominant for soft particles, including emulsion droplets and latex beads.
3. The mechanism of the scattering losses is quite different than the viscous and thermal losses. Acoustic scattering does not produce dissipation of acoustic energy. This mechanism of scattering is similar to that of light scattering. Particles simply redirect a part of the acoustic energy flow and as a result this portion of the sound does not reach the sound transducer. This mechanism is important for larger particles (> 3 μm) and high frequency (> 10 MHz>).
4. The intrinsic losses of the acoustic energy occur due to the interaction of the sound wave with the materials of the particles and medium as homogenous phases on a molecular level.
5. Structural losses are caused by the oscillation of a network of particles that are interconnected. Thus, this mechanism is specific for the given type of structured system.
6. Electrokinetic losses are caused by the oscillation of charged particles in an acoustic field, which leads to the generation of an alternating electrical field, and consequently to an alternating electric current. As a result, a part of the acoustic energy is transformed into electrical energy and then irreversibly to heat.

Only the first four loss mechanisms (viscous, thermal, scattering, and intrinsic) make a significant contribution to the overall attenuation spectra in most cases. Structural losses are significant only in structured systems that require a quite different theoretical framework. These four mechanisms form the basis for acoustic spectroscopy.

The contribution of electrokinetic losses to the total sound attenuation is almost always negligibly small (9) and will be neglected. This opens an opportunity to separate acoustic spectroscopy from electroacoustic spectroscopy because acoustic attenuation spectra are independent of the electric properties of the dispersed system.

Following this distinction between acoustics and electroacoustics, the corresponding theories will be considered separately.

III. THEORY OF ACOUSTICS

The most well known acoustic theory for heterogeneous systems was developed by Epstein and Carhart (3), and Allegra and Hawley (10). This theory takes into account the four most important mechanisms (viscous, thermal, scattering, and intrinsic) and is termed the "ECAH theory." This theory describes attenuation for a monodisperse system of spherical particles and isvalid only for dilute systems.

The term "monodisperse" assumes that all of the particles have the same diameter. Extensions of the ECAH theory to include polydispersity have typically assumed a simple linear superposition of the attenuation for each size fraction. The term "spherical" is used to denote that all calculations are performed assuming that each particle can be adequately represented as a sphere.

Most importantly, the term "dilute" is used to indicate that there is no consideration of particle-particle interactions. This fundamental limitation normally restricts the application of the resulting theory to dispersions with a volume fraction of less than a few volume per cent. However, there is some evidence that the ECAH theory, in some very specific situations, does nevertheless provide a correct interpretation of experimental data, even for volume fractions as large as 30%.

An early demonstration of the ability of the ECAH theory was provided by Allegra and Hawley. They observed almost perfect correlation between experiment and dilute case ECAH theory for several systems: a 20% by volume toluene emulsion; a 10% by volume hexadecane emulsion; and a 10% by volume polystyrene latex. Similar work with emulsions by McClements (11, 12) has provided similar results. The recent work by Holmes *et al*et al. (13, 14) shows good agreementbetween ECAH theory and experiments even for 30% by volume polystyrene latex.

A surprising absence of particle-particle interaction was observed with neoprene latex (15). This experiment showed that attenuation is a linear function of volume fractions up to 30% for this particular system (Fig. 1). This linearity is an indication that each particle fraction contributes to the total attenuation independently of other fractions, and is a superposition of individual contributions. Superposition works only when particle-particle interaction is insignificant.

It is important to note that the surprising validity of the dilute ECAH theory for moderately concentrated systems has only been demonstrated in systems where the "thermal losses" were dominant, such as emulsions and latex systems. In contrast, a solid rutile dispersion exhibits nonlinearity of the attentuation above 10% by volume (Fig. 2).

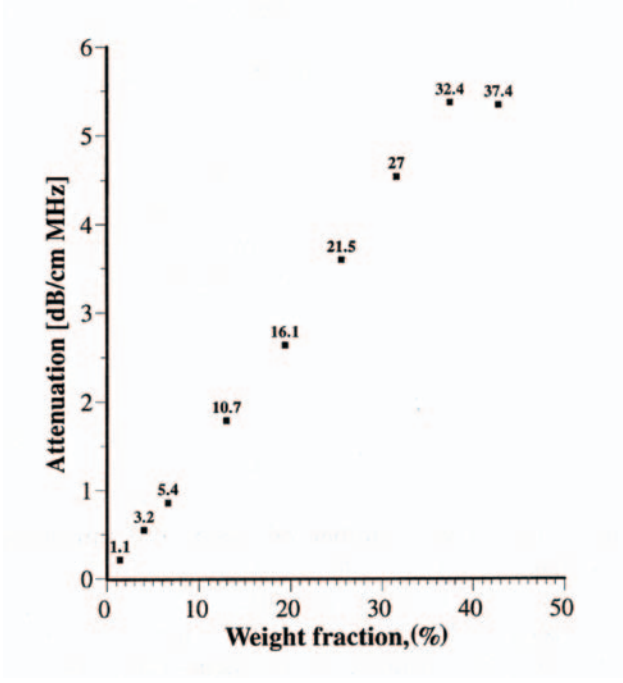

Figure 1 Dependence of attenuation in the neoprene latex at a frequency of 15 MHz) on the dispersed system weight fraction. Corresponding volume fractions in % are shown as the data points labels.

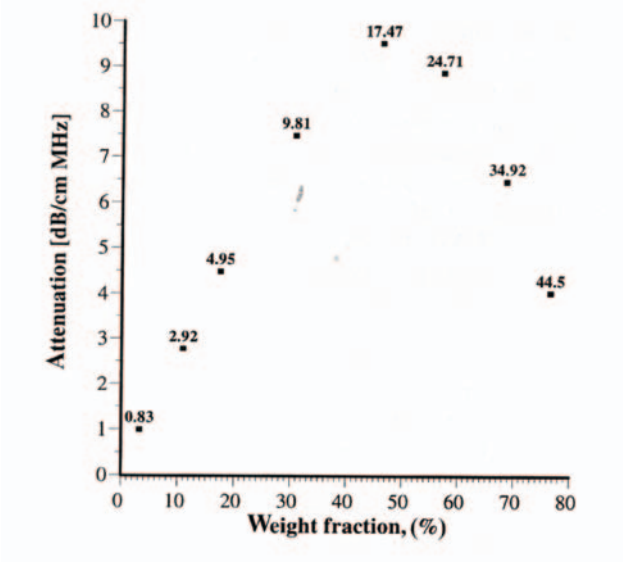

Figure 2 Dependence of attenuation in the rutile dispersion (rutile R-746, DuPont), at a frequency of 15 MHz, on the dispersed system weight fraction. Corresponding volume fractions in % are shown as the data points labels.

The difference between the "viscous depth" and the "thermal depth" provides an answer to the observed differences between emulsions and solid particle dispersions. These parameters characterize the penetra tion of the shear wave and thermal wave, respectively, into the liquid. Particles oscillating in the sound wave generate these waves which damp in the particle vicinity. The characteristic distance for the shear wave amplitude to decay is the "viscous depth" δ_v. The corresponding distance for the thermal wave is the "thermal depth" δ_t. The following expressions give these parameter values in dilute systems:

$$\delta_v = \sqrt{\frac{2v}{\omega}} \quad (1)$$

$$\delta_t = \sqrt{\frac{2_\tau}{\omega \rho C_p}} \quad (2)$$

where N is the kinematic viscosity, ω is the frequency, P is the density, T is the heat conductance, and C_p is the heat capacity at constant pressure.

The relationship between $<\delta_v$ and δ_t has been considered before. For instance, McClements plots "thermal depth" and "viscous depth" versus frequency (4). It is easy to show that "viscous depth" is 2.6 times more than "thermal depth" in aqueous dispersions (15). As a result, the particle viscous layers overlap at a volume fraction lower than that of the particle thermal layers. Overlap of the boundary layers is a measure of the corresonding particle-particle interaction. There is no particle interaction when corresponding boundary layers are sufficiently separated.

Thus, an increase in the dispersed volume fraction for a given frequency first leads to the overlap of the viscous layers because they extend further into the liquid. Thermal layers overlap at higher volume fractions. This means that the particle hydrodynamic interaction becomes more important than the particle thermodynamic interaction at the lower volume fractions.

The 2.6 times difference between δ_v and δ_t leads to a large difference in the volume fractions corresponding to the beginning of the boundary layers' overlap. The dilute case theory is valid for volume fractions smaller than the critical volume fractions φ_v and φ_t. These critical volume fractions are functions of the frequency and particle size. These parameters are conventionally defined from the condition that the shortest distance between particle surfaces is equal to $2\delta_v$ or $2\delta_t$. This definition yields the following expression for the ratio of the critical volume fractions in aqueous dispersions:

$$\frac{\varphi_v}{\varphi_t} = \left(\frac{a\sqrt{\pi f} + 2.6^{-1}}{a\sqrt{\pi f} + 1} \right) \quad (3)$$

where a is the particle radius in micrometers, and f is the frequency is in megahertz.

The ratio of the critical volume fractions depends on the frequency. For instance, for neoprene latex, the critical "thermal" volume fraction is 10 times higher than the critical "viscous" volume fraction for 1 Mhz and only three times higher for 100 Mhz.

It is interesting that this important feature of the "thermal losses" works for almost all liquids. We have more than 100 liquids with their properties in our database. The core of this database is the well known paper by Anson and Chivers (16). We can introduce a parameter referred to as the "depth ratio":

$$depth\ ratio = \frac{\delta_v}{\delta_t}$$

This parameter is 2.6 for water, as was mentioned before. Figure 3 shows values of this parameter for all liquids from our database relative to the viscous depth of water. It is seen that this parameter is even larger for many liquids.

Therefore, "thermal losses" are much less sensitive than "viscous lossess" to the particle-particle interaction for almost all known liquids. It makes ECAH theory valid in a

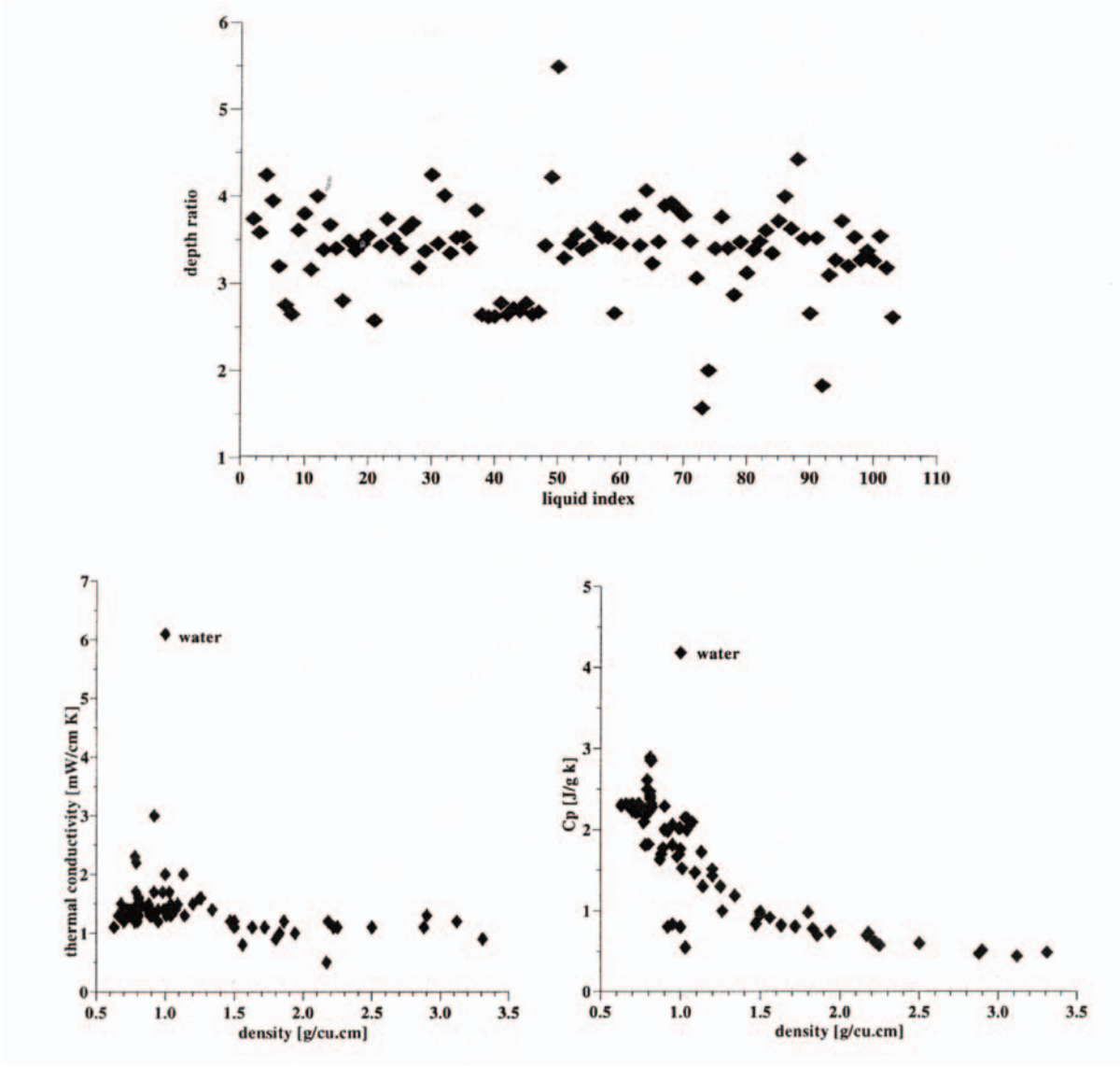

Figure 3 Thermal properties of various liquids.

much wider range of emulsion volume fractions than one would expect.

There is one more fortunate fact for ECAH theory that follows from the values of the liquid's thermal properties. In general, ECAH theory requires information about three thermodynamic properties: thermal conductivity τ, heat capacity C_p, and thermal expansion β. It turns out that × and Cp are almost the same for all liquids except water. Figure 3 illustrates the variation of these parameters for more than 100 liquids from our database. This reduces the number of required parameters to one-thermal expansion. This parameter plays the same role in "thermal losses" as density does in "viscous losses."

ECAH theory has the great disadvantage of being mathematically complex. It cannot be generalized for particle-particle interactions. This is not important, as we have found for emulsions, but may be important for latex systems, and is certainly very important for high-density contrast systems. There are two ways to simplify this theory by using a restriction on the frequency and particle size. The first one is the so-called" long wave requirement" (10) which requires the wavelength of the sound wave λ to be larger than particle radius *a*. This "long-wave requirement" restricts the particle size for a given set of frequencies. Our

experience shows that particle size must be below 10 μm for the frequency range 1-100 MHz. This restriction is helpful for characterizing small particles.

The long-wave requirement provides a sufficient simplification of the theory for implementing particle-particle interactions. It has been done in the work in Ref. 20 on the basis of the "coupled phase model" (18, 19). This theory (19) works up to 40% volume even for heavy materials including rutile.

There is another approach to acoustics which employs a "short-wave requirement." It was introduced by Riebel et al. (20). This approach works only for large particles (above 10 um, but requires only limited input data on the sample. The theory may provide an important advantage in the case of emulsions and latex systems when the thermal expansion is not known.

Thre is opportunity in the future to create a mixed theory that could use a polynomial fit merging together "short" and "long" wave range theories. Such a combined theory will be able to cover a complete particle size range from nanometers to millimeters for concentrated systems.

There are two recent developments in the theory of acoustics which deserve to be mentioned here. The first one is a theory of acoustics for flocculated emulsions (21). It is based on EC AH theory, but it uses an addition an "effective medium" approach for calculating thermal properties of the floes. The success of this idea is related to the feature of the thermal losses that allows for insignificant particle - particle interactions even at high volume fractions. This mechanism of acoustic energy dissipation does not require relative motion of the particle and liquid. Spherical symmetrical oscillation is the major term in these kinds of losses. This provides the opportunity to replace the floe with an imaginary particle, assuming a proper choice of the thermal properties.

Another significant development is associated with the name of Samuel Temkin. He offers in his papers (22, 23) a new approach to acoustic theory. Instead of assuming a model dispersion consisting of spherical particles in a Newtonian liquid, he suggests that the thermodynamic approach be explored as far as possible. This very promising theory operates with notions of particle velocities and temperature fluctuations, and yields some unusual results (22, 23). It has not yet been used, as far as we know, in commercially available instruments.

IV. THEORY OF ELECTROACOUSTICS

Whereas acoustic spectroscopy describes the combined effect of the six separate loss mechanisms, electroacoustic spectroscopy, as it is presently formulated, emphasizes only one of these interaction mechanisms, the electrokinetic losses.

In acoustic spectroscopy sound is utilized as both the excitation and the measured variable, and therefore there is but one basic implementation. In contrast, electroacoustic spectroscopy deals with the interaction of electric and acoustic fields and therefore there are two possible implementations. One can apply a sound field and measure the resultant electric field which is referred to as the colloid vibration potential (CVP), or conversely one can apply an electric field and measure the resultant acoustic field which is referred to as the ESA.

First, let us consider the measurement of CVP. When the density of the particles P_p differs from that of the medium P_m, the particles move relative to the medium under the influence of an acoustic wave. This motion causes a displacement of the internal and external parts of the double layer (DL). The phenomenon is usually referred to as a polarization of the DL (6). This displacement of opposite charges gives rise to a dipole moment. The superposition of the electric fields of these induced dipole moments over the collection of particles gives rise to a macroscopical electric field which is referred to as the colloid vibration potential (CVP). Thus, the fourth mechanism of particles' interaction with sound leads to the transformation of part of the acoustic energy to electrical energy. This electrical energy may then be dissipated if the opportunity for electric current flow exists.

Now let us consider the measurement of ESA which occurs when an alternating electric field is applied to the disperse system (7). If the zeta potential of the particle is greater than zero, then the oscillating electrophoretic motion of the charged dispersed particles generates a sound wave.

Both electroacoustic parameters CVP and ESA can be experimentally measured. The CVP or ESA spectrum is the experimental output from electroacoustic spectroscopy. Both of these spectra contain information on the zeta potential and particle size distribution (PSD); however, only one of the electroacoustic spectra is required because both of them contain essentially the same information about the dispersed system.

The conversion of electroacoustic spectra into PSD requires a theoretical model of the electroacoustic phenomenon. This conversion procedure is much more complicated for electroacoustics than for acoustics. The reason for the additional problems relates to the additional field involved in the characterization, i.e., the electric field. The theory becomes much more complicated because of this additional field.

For some time, O'Brien's theory (24, 25) has been considered as a basis for electroacoustics, including concentrated systems. For instance, the review of electroacoustics published by Hunter (7) mentions a somewhat modified version of O'Brien's theory for the electroacoustic characterization of emulsions. However, a few papers have appeared recently (26-28) which express some doubts in O'Brien's theory. It is shown in these papers that O'Brien's theory contradicts the Onsager principle if applied to concentrated systems. There is also a large discrepancy between this theory and experiment. These newpapers offer a different electroacoustic theory which is supposed to be valid in concentrates. In particular, this theory gives correct interpretation of the two equilibrium dilution tests with small silica (30 nm) and larger rutile (300 nm) particles. In both cases the theory works with concentrates (up to 40% by volume) of rutile, for instance.

So far, this new electroacoustic theory has been tested with rigid heavy particles only. It is not clear yet how it will work with emulsions as there were no experimental data for emulsions available. This concern is related to the fact that this theory as well as O'Brien's theory neglect thermodynamic effects. It is rather surprising, keeping in mind that the thermodynamic effect of "thermal losses" is dominant for the acoustics of emulsions. It is not yet clear why electro acoustics is so different from acoustics in that thermo dynamic effects are not important.

We offer one simple hypothesis that might explain this difference. Electroacoustics is related to the displacement of the electric charges in the DL. This displacement is characterized by dipole symmetry. At the sametime "thermal losses" measured by acoustics are associated mostly with spherical symmetry. They are caused by oscillation of the particle's volume in the sound wave. It is clear that such a spherically symmetrical oscillation does not cause displacement of electric charges in DLs with dipole structure.

This is a hypothesis and a fundamental theory that will take into account thermodynamic effects in addition to electrodynamic and hydrodynamic effects which should resolve the question. The electroacoustic theory of emulsions will not be complete unless such a theory is developed. Nevertheless, electroacoustics, even at the present stage, can yield very important information about electric surface properties of emulsions as it will be shown below.

V. BUBBLES PROBLEM

One of the experimental problems that may affect acoustics is the presence of air bubbles during measurements. While bubbles will affect sound attenuation and speed, it is worth considering how much of an effect they really have and whether the bubbles will detract from the acoustic techniques:

1. It has been determined that acoustic spectra are affected by bubbles. An acoustic theory describing sound propagation through bubbly liquid was developed by Foldy in 1944 (29), and confirmed experimentally in the 1940s and 1950s (30, 31).
2. The contribution of bubbles to sound speed and attenuation depends on the bubble size and sound frequency. For instance, a 100-μm bubble has a resonance frequency of about 60 kHz. This frequency is reciprocally proportional to the bubble diameter. A bubble of 10 μm diameter will have a resonance frequency of about 0.6 MHz.
3. Acoustic spectroscopy of dispersed systems operates with frequencies above 1 MHz and usually up to 100 MHz. The size of the bubbles must be well below 10 μm in order to affect the complete frequency range of the acoustic spectrometer.
4. Bubbles with sizes below 10 μm are very unstable as is known from general colloid chemistry and the theory of notation. "Colloid-sized gas bubbles have astonishingly short lifetimes, normally between 1 μs and 1 ms" (32). They simply dissolve in li.quid because of their high curvature.

Bubbles can only affect the low-frequency part of the acoustic spectra (below 10 MHz). The frequency range 10-100 MHz is available for particle characterization even in the bubbly liquids. Acoustic spectrometers can both sense bubbles and characterize particle size. We can confirm this conclusion with thousands of measurements performed with hundreds of different systems. Sensitivity to bubbles, in fact, is an important advantage of acoustics over electroacoustics. The presence of bubbles may affect the properties of the solid dispersed phase. For instance, bubbles can be centers of aggregation, which makes them an important stability factor.

VI. MEASURING TECHNIQUE

Currently, there are three acoustic spectrometers on the market: Ultrasizer from Malvern, Opus of Sympatec, and

DT-100 from Dispersion Technology. All of them are claimed to be able to characterize emulsions in the wide droplet size range. There are some major differences between them. For instance, Opus was designed initially for large particles only because it employs the "short wavelength requirement" (21).

There are also two electroacoustic spectrometers on the market: the AcoustoSizer from Colloidal Dynamics and the DT-200 from Dispersion Technology. There is only one instrument which provides both features, acoustics and electroacoustics together, and this is the DT-1200 Acoustic and Electroacoustic Spectrometer from Dispersion Technology.

Comparison of the different instruments lies beyond the scope of this review. The Dt-1200 was used for all experiments described in this work. A description of this instrument is given below.

The DT-1200 has two separate sensors for measuring acoustic and electroacoustic signals separately. Both sensors use the pulse technique. The acoustic sensor has two piezo crystal transducers. The gap between the transmitter and receiver is variable in steps. In default mode, the gap changes from 0.15 mm up to 20 mm in 21 steps. The basic frequency of the pulse changes in steps as well. In default mode, the frequency changes from 3 to 100 MHz in 18 steps. The number of pulses collected for each gap and frequency is automatically adjustable in order to reach the target signal-to-noise ratio.

The variable-gap technique is an essential feature of the acoustic spectrometer. This makes it possible to cover a wide dynamic range of possible attenuations. For instance, pure water is almost transparent to ultra sound at a low frequencies (below 10 MHz). The attenuation of water reaches only 5 dB/cm at 50 MHz. Therefore, the attenuation of water should be measured at large gaps, as little information is obtained from small gaps.

Water is the least attenuating liquid known to us. In contrast, a 40% by weight water-in-cyclo methicone emulsion attenuates ultrasound very strongly (Fig. 4). This attenuation reaches 450 dB/cm 50 MHz. Thisoccurs because cyclo methicone has a very high thermal expansion coefficient of $14.5\ 10^{-4}\ 1K^{0}$. The acoustic attenuation results for this system can only be obtained at small gaps. At larger gap size, the ultrasound signal simply does not pentrate to the receiver because of the high attenuation.

The acoustic sensor measures also sound speed at a single chosen frequency. The sound speed is measured by recording the time it takes for a pulse to arrive at the receiver. The instrument automatically adjusts the pulse sampling, depending on the value of the sound speed. An accurate knowledge of the sound speed is necessary for eliminating possible artifacts such as excessive attenuation at low frequencies.

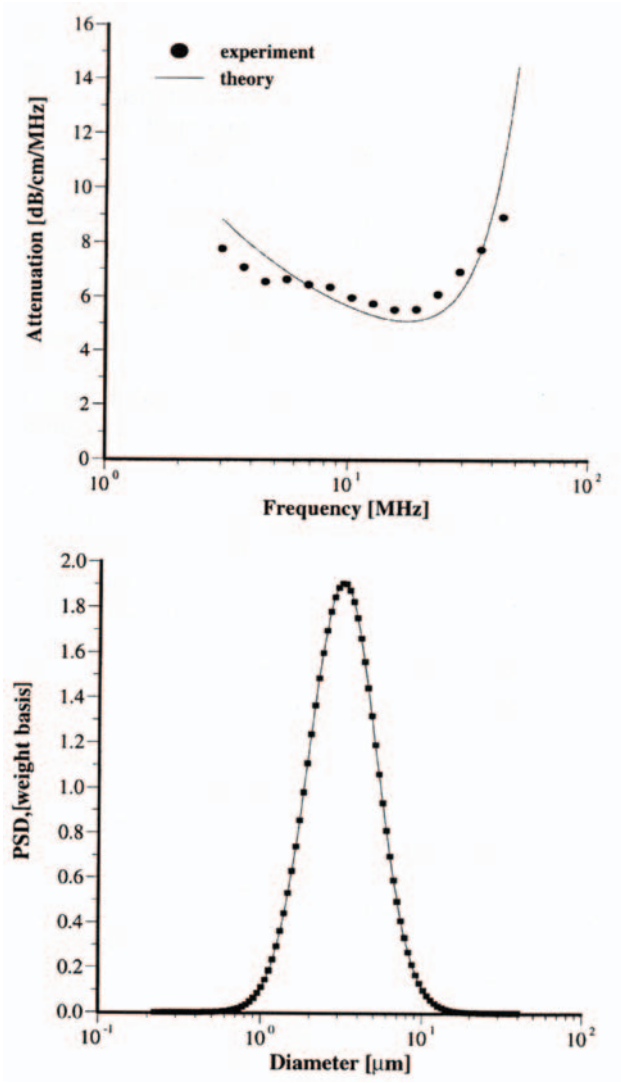

Figure 4 Attenuation spectra and droplet size distribution of 40% water in cyclo methicone emulsion.

Sound-speed measurement is especially critical for characterizing emulsions. There are considerable data indicating that the sound speed of various liquids is extremely dependent on small traces of contamination. Examples of such complex behavior of different mixed liquids is given

in the literature (33). Figure 5 illustrates one of the examples from this book. Therefore, the only reliable way to obtain the sound speed of a given emulsion is by experimental measurement. This is important to keep in mind when evaluating different acoustic instrument models as an instrument without the capability to measure sound speed is very limited.

The DT-1200 instrument is able to measure sound speed quite reliably, which is is illustrated in Fig. 6 showing the results of a dilution test with silica Ludox TM. The experimentally measured sound speed was found to be very close to theoretical calculations.

The electroacoustic sensor measures the magnitude and phase of the CVC at 1.5 and 3 MHz. It has a piezo crystal sound transmitter and a specially designed electric antenna. The distance between the transmitter and antenna is 5 mm. There is a provision for automatic correction of the sound speed and attenuation measured with the acoustic sensor.

There is a special analysis program which calculates (PSD) from attenuation spectra and zeta potential from the CVC. This program uses the ECAH theory for calculating "thermal losses", the Waterman-Truell theory (34) for calculating scattering losses, and the theory described in the Ref. 19 for calculating viscous losses. The electroacoustic theory used with the new version of the instrument is described in Ref. 28.

This program tests lognormal, bimodal, and modified lognormal (35) PSDs. It uses an error analysis in order to search for the best PSD. The goal of the optimization procedure is to minimize the error of the theoretical fit to the experimental attenuation spectra.

The analysis program takes into account the PSD correction when it calculates zeta potential. It uses either PSD calculated from the attenuation spectra or a priori known PSD. The analysis routine also makes a correction for attenuation of the sound pulse.

The total required sample volume is about 100 ml. There is a special magnetic stirrer preventing sedimentation and promoting mixing of chemicals during titration. The instrument has two burets and appropriate software for automatic

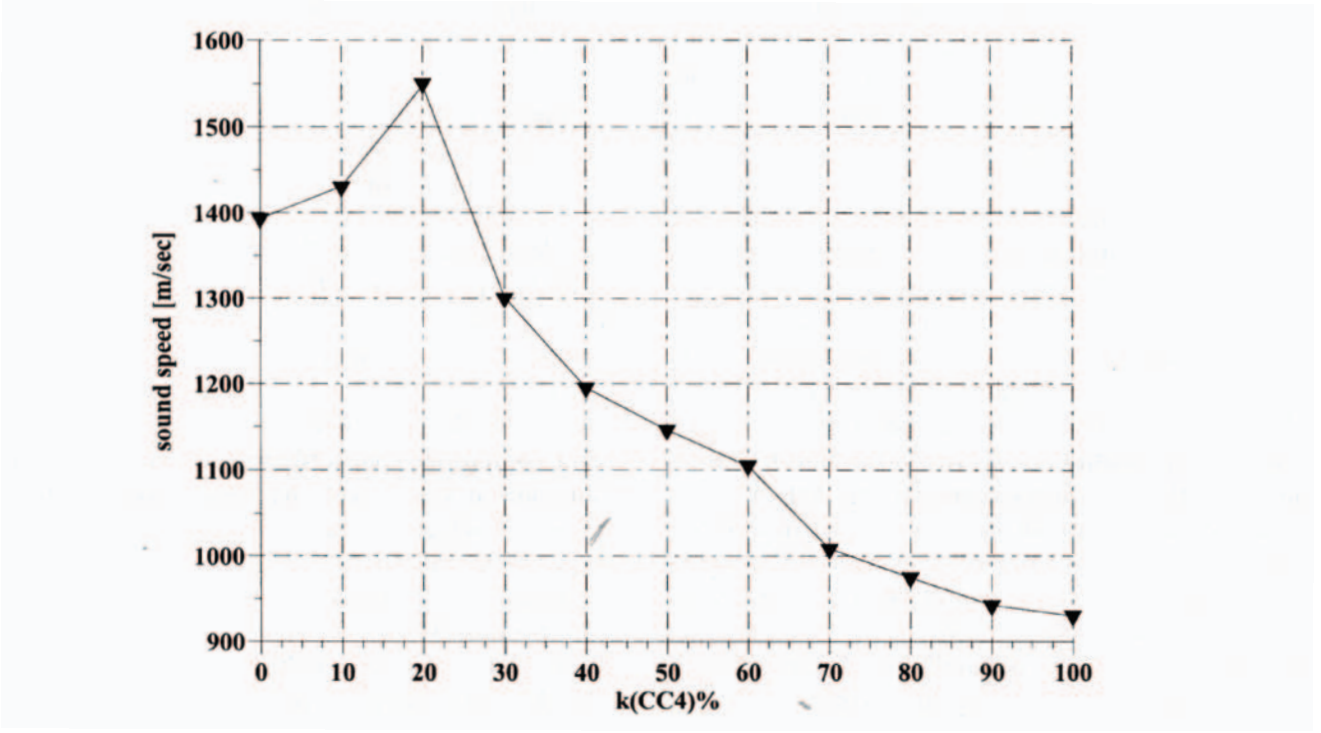

Figure 5 Sound speed of water-CC_4 mixture.

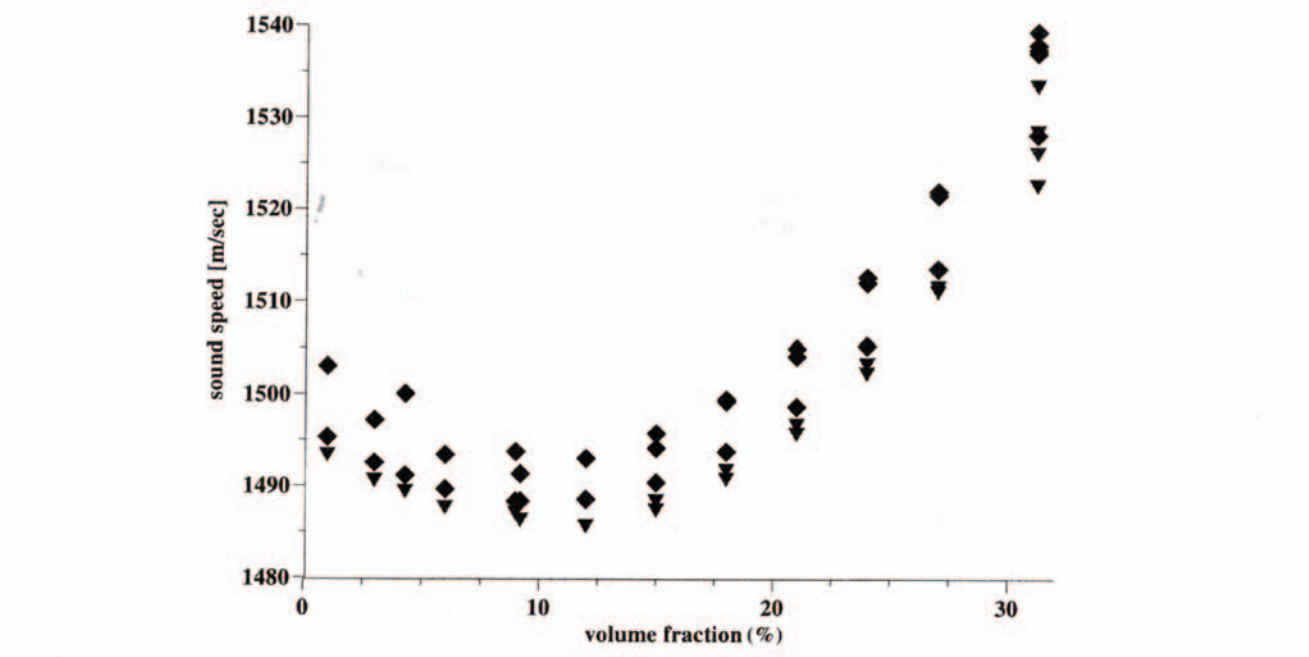

Figure 6 Sound speed for silica Ludox TM vs. volume fraction. Equilibrium dilution using dialysis. Theory (triangles) according to the Wood expression; experiment diamonds.

titration. Conductivity and temperature probes are also available.

One attenuation spectra measurement with a default set-up takes from 5 to 10 min. A user can speed up the measurement by changing set-up parameters. One CVC measurement takes from 10 s to 1 min depending on the system properties.

The precision and accuracy of the DT-1200 for emulsions are described below. We start here with solid particles because it is much easier to test the reproducibility and accuracy with a stable dispersion of solid particles (36). Possible variation of the emulsion droplets can affect this test.

The attenuation spectra in Fig. 7 provide an example of the acoustic sensor precision. These attenuation spectra were measured using alumina Sumitomo AA-2 and silica Ludox TM. The alumina sample was measured 10 times repeatedly while the silica sample was measured 11 times repeatedly. The corresponding median particle size results are given in Table 1.

The absolute variation of the median particle size was 0.9% for alumina and 1.5% for silica. These values show the precision of the acoustic sensor.

Figures 8 and 9 illustrate the precision of the electroacoustic sensor. Figure 8 provides results for 51 continuous CVC measurements on silica Ludox. The precision measured as the absolute variation of the zeta potential measurement is a fraction of a millivolt. Figure 9 shows titration curves for two different silica samples.

The accuracy characterizes correlation between real and measured values. The accuracy of PSD measurements is a measure of the adequacy of the measured PSD. In order to determine the accuracy of the PSD, one needs a standard system with a known particle size distribution. BCR silica quartz was chosen as a standard with a median size of about 3 urn. This system was chosen because it is a well-known PSD standard in Germany.

Figure 10 shows the standard particle size distribution and PSD measured with the DT-1200. The difference in the median particle size between the standard and experimental results obtained with the DT-1200 was less than 1 %. The PSD was also found to contain a higher percentage of the smaller particles and this gave an accuracy of 5% for the standard deviation (measure of polydispersity).

A test of the measurement accuracy of zeta potential is much more complicated because there is no zeta potential standard for concentrated systems. The absence of electroacoustic theory for concentrated systems creates additional complexity. Our experience is that CVC makes it possible to measure ζ with almost the same accuracy as micro-electrophoresis.

We have also tested the accuracy and precision of the D-1200 Acoustic Spectrometer using Standard Dow Latex with an expected median particle size of 0.083 μm. The results are shown in Table 2.

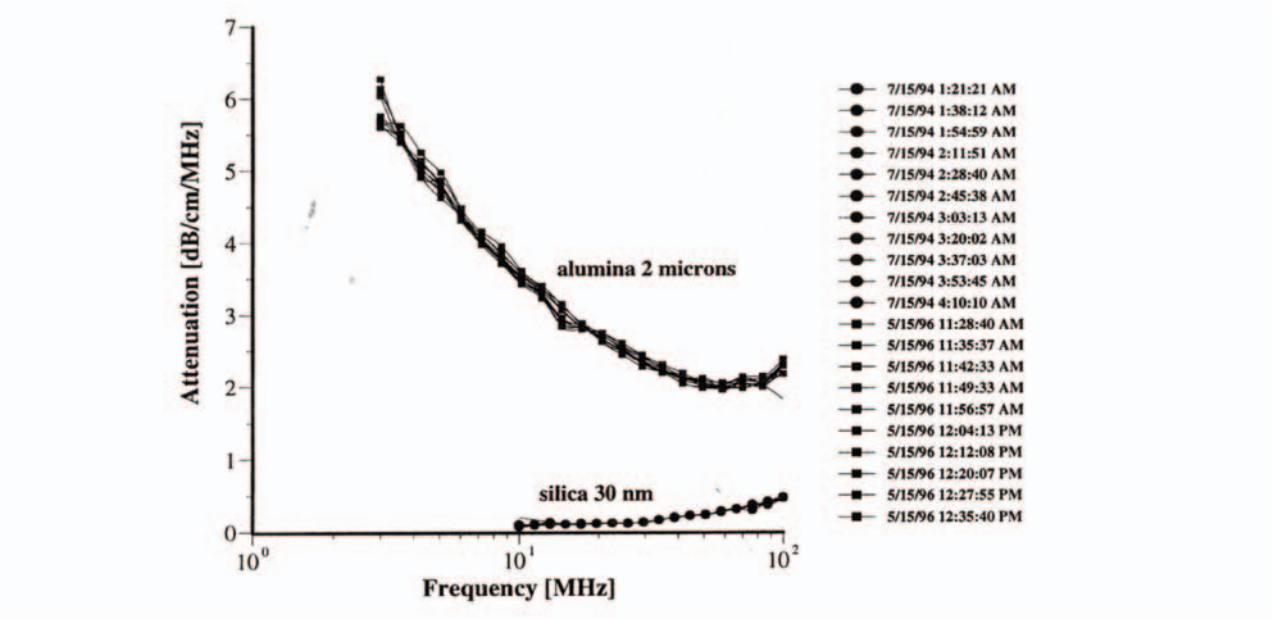

Figure 7 Attenuation of the multiple measurements with alumina Sumitomo AA-2 and silica Ludox TM at 10% wt.

Table 1 Median Particle Size (μm)

Alumina	2.015	2.076	2.057	2.092	2.065	2.047	2.035	2.075	2.039	2.085	
Silica	0.03	0.029	0.029	0.029	0.029	0.03	0.03	0.029	0.03	0.03	0.03

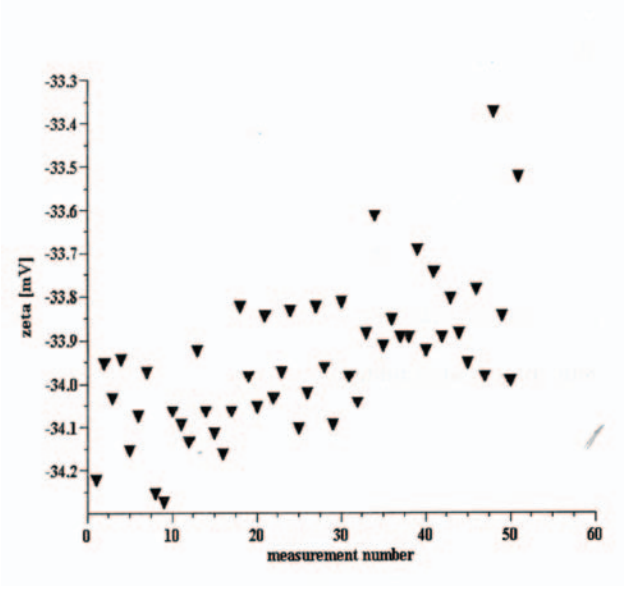

Figure 8 Multiple ζ-potential measurements of 10% wt silica Ludox.

VII. APPLICATIONS AND EXPERIMENTS

A. Emulsions

There are many instances of successful characterization of the PSD and zeta potential of emulsion droplets. There are two quite representative reviews of these experiments published by McClements (4) (acoustics) and Hunter (8) (electroacoustics).

Some results of our recent investigation are presented that were not published before. Various factors that affected stability, size, and zeta potential of the emulsion droplets were investigated.

The first experiment was a repetition to some extent of McClements' work with hexadecane-in-water emulsions. An emulsion was prepared following McClements work (37), containing 25% by weight of hexadecane in water. The measured attenuation spectra (Fig. 11) exhibited a pronounced time dependence. The sound attenuation was found to increase in magnitude as time elapsed. This increase in the attenuation corresponded to the droplet popu-

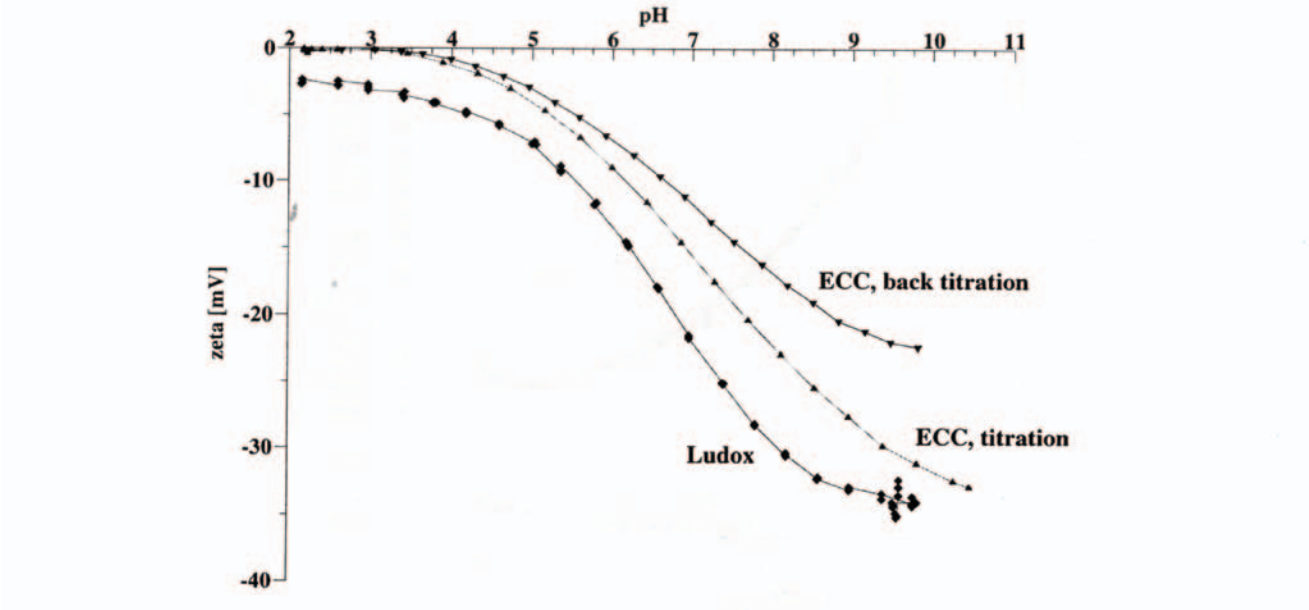

Figure 9 Titration of silica Ludox TM at 10% wt and chemical-mechanical polishing silica ECC.

lation becoming smaller in size. The median droplet size was reduced by almost half during a half-hour experiment. This reduction in droplet size was caused by the shear induced by a magnetic stirrer used in the sample chamber of the DT-1200 instrument. As the emulsion was stirred, the larger drops were fragmented into smaller droplets.

Another important parameter affecting emulsions is the surfactant concentration that affects surface chemistry. This factor was tested for reverse water-in-oil emulsion. The oil phase was simply commercially available car-lubricating oil diluted twice with paint thinner in order to reduce the viscosity of the final sample. Figure 12 illustrates results for emulsions prepared with 6% by weight of water.

This figure shows the attenuation spectra for three samples. The first sample was a pure oil phase and exhibited the lowest attenuation. It is important to measure the attenuation of the pure dispersion medium when a new liquid is evaluated. In this particular case, the intrinsic attenuation of the oil phase was almost 150 dB/cm at 100 MHz which is more than seven times higher than for water. This intrinsic

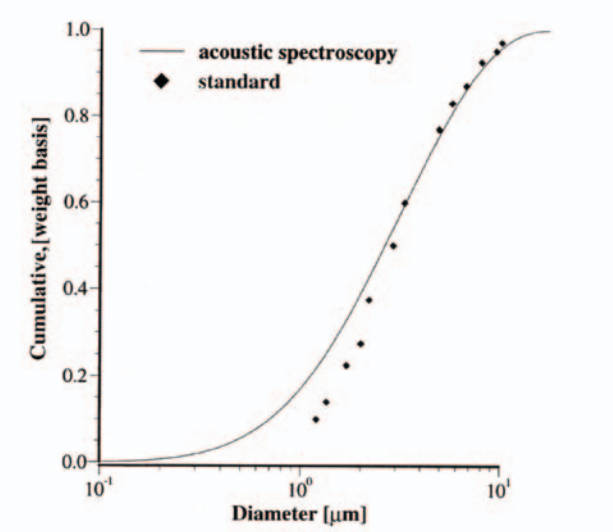

Figure 10 Particle size distribution (PSD) of the silica quartz BCR. Acoustic measurement has been performed with an 11 % wt in ethanol.

Table 2 Median Diameter Measured for 10% wt Latex Serva 44405, Standard Dow Latex with Expected Median Size of 0.083 μm

	1	2	3	4	5	6	7	8	9	10
Median diameter μm	0.0767	0.0765	0.0867	0.0823	0.0775	0.0737	0.0713	0.081	0.076	0.075

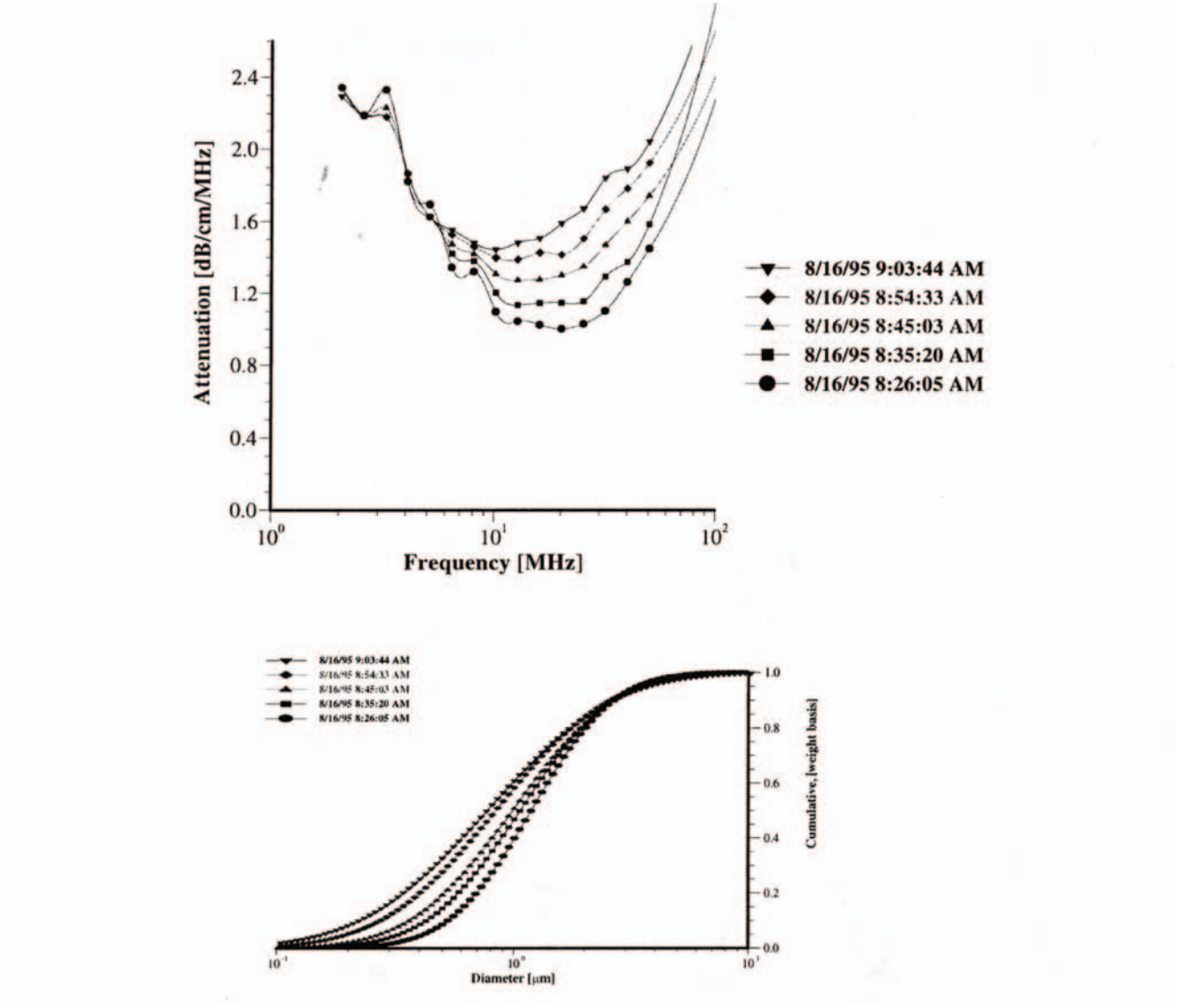

Figure 11 Attenuation and corresponding PSD of 25% wt hexadecane-in-water emulsion.

attenuation is a very important contribution to the attenuation of ultrasound in emulsions. It is the background for characterizing emulsion systems.

The emulsion without added surfactant was measured twice with two different sample loads. As the water content was increased the attenuation became greater in magnitude. For this system, the attenuation was found to be quite stable with time. Addition of 1% by weight of AOT [sodium bis (2-ethylhexylsulfosuccinate] changed the attenuation spectra dramatically. This new emulsion with modified surface chemistry was measured twice in order to show reproducibility. The corresponding PSD is shown in Fig. 12 and indicates that the AOT converted the regular emulsion into a microemulsion as one could expect.

These experiments proved that the acoustic technique is capable of characterizing the PSD of relatively stable emulsions. In many instances, emulsions are found that are not stable at the dispersed volume concentration required to obtain sufficient attenuation signals (usually above 0.5%). Hazy water in fuel emulsions (diesel, jet fuel, gasoline) may exist at low water concentrations of only a few 100 ppmv (0.01%) of dispersed water. Attempts at characterizing

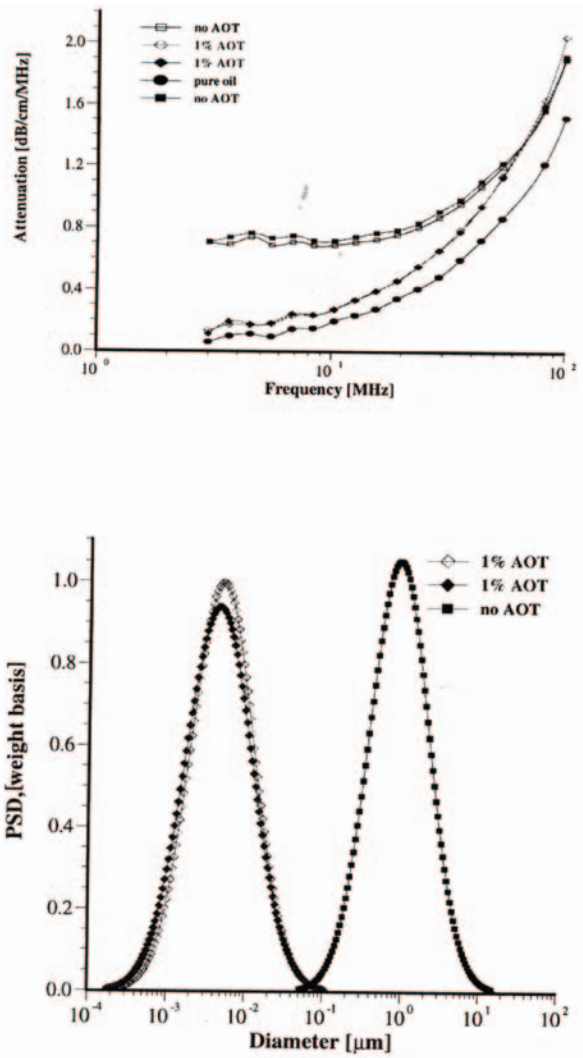

Figure 12 Attenuation and corresponding PSD of 6% wt water-in-car-oil emulsion and microemulsion caused by AOT.

these systems without added surfactant resulted in unstable attenuation spectra, and water droplets were discovered to separate from the bulk emulsion and settle out on the chamber walls. This problem is less important for thermodynamically stable microemulsions.

B. Microemulsions

The mixture of heptane with water and AOT is a classic three-component system. It has been widely studied due to a number of interesting features it exhibits. This system forms stable reverse mciroemulsions (water in oil) without the complication introduced by additional cosurfactant. Such a cosurfactant (usually alcohol) is required by many other reverse microemulsion systems. This simplification makes the alkane/water/AOT system a model for studying reverse microemulsions.

There have been many studies devoted to characterization of these practically important systems. Reverse emulsion droplets have been used as chemical micro-reactors to produce nanosize inorganic and polymer particles with special properties that are not found in the bulk form (38-42). These microemulsion systems have also been a topic of research for biological systems and the AOT head groups have been found to influence the conformation of proteins and increase enzyme activity (43-6). The unique environment created in the small water pools of swollen reverse micelles allows for increased chemical reactivity. The increase in surface area with decreased in size of the droplets also can significantly increase reactivity by allowing greater contact of immiscible reactants.

There have been many attempts to measure the droplet size of ths microemulsion. Several different techniques were used: PCS (47-52), classic light scattering (49, 51, 53), neutron scattering (SANS) (54-56), X-ray scattering (SAXS) (48, 57, 58), ultracentrifugation (46, 50, 53), and viscosity (48, 50, 53). It was observed that the heptane/water/AOT microemulsions have water pools with diameters ranging from 2 nm up to 30 nm. The water drops are encapsulated by the AOT surfactant so that virtually all of the AOT is located at the interface shell. The size of the water droplets can be conveniently altered by adjusting the molar ratios of water to surfactant designated as$R$ R ([H2O]/[AOT]). At low R values ($\leq$ 10) the water is strongly bound to the AOT surfactant polar head groups and exhibits unique characteristics different from bulk water (53). At higher water ratios ($R > 20$), free water is predominant in the swollen reverse micellular solutions, and at approximately $R = 60$, the system undergoes a transition from a transparent microemulsion into an unstable turbid macroemulsion. This macroemulsion separates on standing into a clear upper phase and a turbid lower phase.

The increase in droplet size and phase boundary can also be achieved by raising the temperature up to a critical value of 55°C. In adition, this system has been found to exhibit an electrical percolation threshold whereby the conductivity increases by several orders of magnitude by either varying the R ratio or increasing the temperature (56, 57, 59, 60). Despite all these efforts, there still remain questions regarding the polydispersity of the water droplets, and few studies are available above the R value of 60 where a turbid macroemulsion state exists.

Acoustic spectroscopy offers a new opportunity for characterizing such complicated systems. Details of this experiment are presented in the Ref. 61. The reverse microemulsions were prepared by first making a 0.1 M solution of AOT in heptane (6.1% wt AOT). The heptane was obtained from Sigma as HPLC grade (99 + % purity). Known amounts of 18 MΩ cm water were added to the AOT-heptane solution using a 1 ml total volume graduated glass syringe and then shaken for 30 s in Teflon-capped glass bottles. The shaking action was required to overcome an energy barrier to distribute the water into the nanosized droplets, as it could not be achieved using a magnetic stirrer.

In all cases, the reported R values was based on the added water, and were not corrected for any residual water that may have been in the dried-AOT or heptane solvent. Karl Fischer analysis of the AOT-heptane solutions before the addition of water resulted in an R value of 0.4. This amount was considered to be negligible.

Measurements were made starting with the pure water and heptane and then the AOT-heptane sample with no added water ($R = 0$). The sample fluid was removed from the instrument cell and placed in a glass bottle with a Teflon cap. Additional water was titrated and the microemulsion was shaken for 30 s before being placed back in the instrument cell. The sample cell contained a cover to prevent evaporation of the solvents. The samples were visually inspected for clarity and rheological properties for each R value. These steps were repeated for increasing water weight fraction or R ratios up to 100. At $R \geq 60$ the microemulsions became turbid. At $R > 80$, the emulsions became distinctly more viscous.

The weight fractions of the dispersed phase were calculated for water only, without including the AOT. Each trial run lasted approximately 5-10 min with the temperature varied from 25-27°C. A separate microemulsion sample for $R = 4$- was made up a few days before the first study. For the $R = 70$ sample, a second acoustic measurement was carried out with the same sample used for the first study. The complete set of experiments for water, heptane, and the reverse microemulsions from $R = 0$ to 100 was repeated to evaluate the reproducibility.

Attenuation spectra measured in the first run up to $R = 80$ are presented in Fig. 13. The results for $R = 90$ and $R = 100$ are not reported because they were found to vary appreciably. As the water concentration is increased, the attenuation spectrum rises in intensity and there is a distinct jump in the attenuation spectrum from $R = 5$- to $R = 60$ in the low-frequency range. This discontinuity is also reflected in the visual appearance, as at $R = 60$ the system becomes turbid. The smooth shape of the attenuation curve also

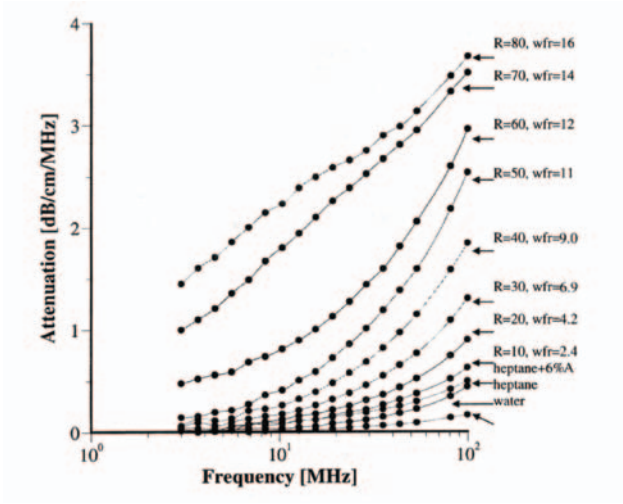

Figure 13 Acoustic attenuation spectra measured for water/AOT/heptane system for different water-to-AOT ratios R.

changes at $R > 60$. The stability and reproducibility of the system was questioned owing to the irregular nature of the curve, so the experiment at $R = 70$ was repeated and gave almost identical results. An additional experiment was run at $R = 40$ for a separate microemulsion prepared a few days earlier. This showed excellent agreement with the results for freshly titrated microemulsion.

For R values > 70, an increase in the viscosity and a decrease in the reproducibility of the attenuation measurement were observed. This could be due to the failure of the model of this system as a collection of separate droplets at high R values.

A second set of experiments was run to check the reproducibility. The results of both sets of experiments up to $R = 60$ are given in Fig. 14. It can be seen that the error related to the reproducibility is much smaller than the difference between attenuation spectra for the different R values. This demonstrates that the variation of attenuation reflects changes in the sample properties of water weight fraction and droplet size. The sound attenuation at R values above 60 were not as reproducible, but did give the same form of a bimodial distribution as the best fit for the experimental data.

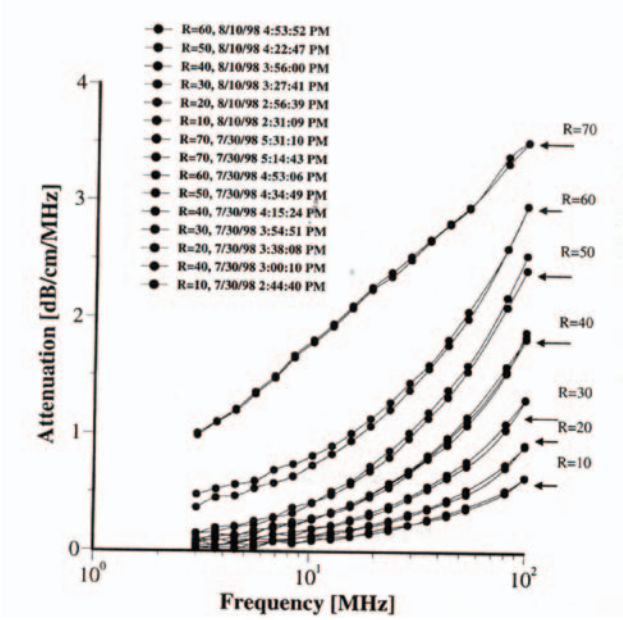

Figure 14 Reproducibility test of the attenuation measurement.

The two lowest attenuation curves correspond to the attenuation in the two pure liquids: water and heptane. This attenuation is associated with oscillation of liquid molecules in the sound field. If these liquids are soluble in each other, the total attenuation of the mixture would lie between these two lowest attenuation curves. However, it can be seen that the attenuation of the mixture is much higher than that of the pure liquids. The increase in attenuation is, therefore, due to this heterogeneity of the water in the heptane system. The extra attenuation is caused by motion of droplets, not separate molecules. The scale factor (size of droplets) corresponding to this attenuation is much higher than that for pure liquids (size of molecules).

The current system contains a third component AOT. A question arises on the contribution of AOT to the measured attenuation. In order to answer this question, measurements were performed on a mixture of 6.1% by weight. AOT in heptane ($R = 0$). It is the third smallest attenuation curve in Fig. 13. It is seen that attenuation increases somewhat due to AOT. However, this increase is less than the extra attenuation produced by water droplets. The small increase in attenuation is attributed to AOT micelles. Unfortunately the thermal properties of AOT as a liquid phase are not known and the size of these micelles could not be calculated.

The PSDs corresponding to the measured attenuation spectra are prsented in Fig. 15. It can be seen that the distribution becomes bimodal for $R \geq 60$, which coincides with the onset of turbidity. It is to be noted that such a conclusion could not easily be arrived at with other techniques. However, Fig. 15 illustrates a peculiarity of this system that can be compared with independent data from the literature (54, 55): mean particle size increases with R in an almost linear fashion. This dependence becomes apparent when mean size is plotted as a function of R as in Fig. 16.

It is seen that mean particle sizes measured used acoustic spectroscopy are in good agreement with those obtained independently using the SANS and SAXS techniques (43, 48, 54) for R values ranging from 20 to 60. A simple theory based on equipartition of water and surfactant (36) can reasonably explain the observed linear dependence.

At $R = 10$ the acoustic method gave a slightly larger diameter than expected. This could be as a result of the constrained state of the "bound water" in the swollen reverse micelles. The water under these conditions may exhibit different thermal properties from those of the bulk water used in the particle size calculations. Also, at the low R values ($R \leq 10$ or $\leq 2.4\%$ water), the attenuation spectrum is not very large as compared to the background heptane signal.

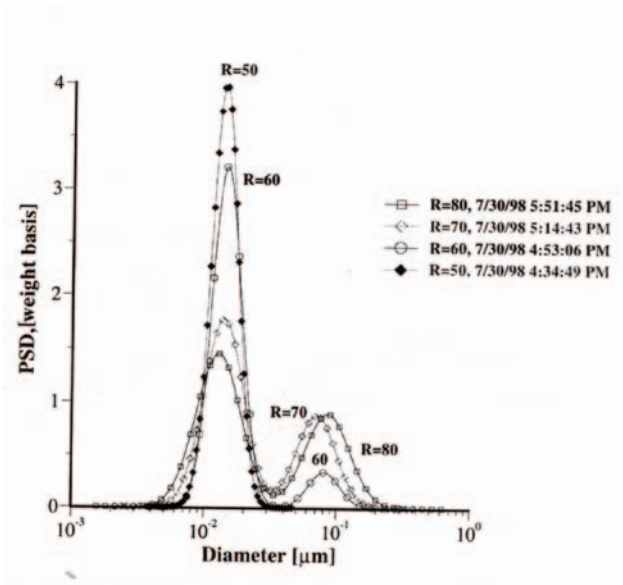

Figure 15 Drop size distribution for varying R [H20]/[AOT] from 10 to 50 and from 50 to 80.

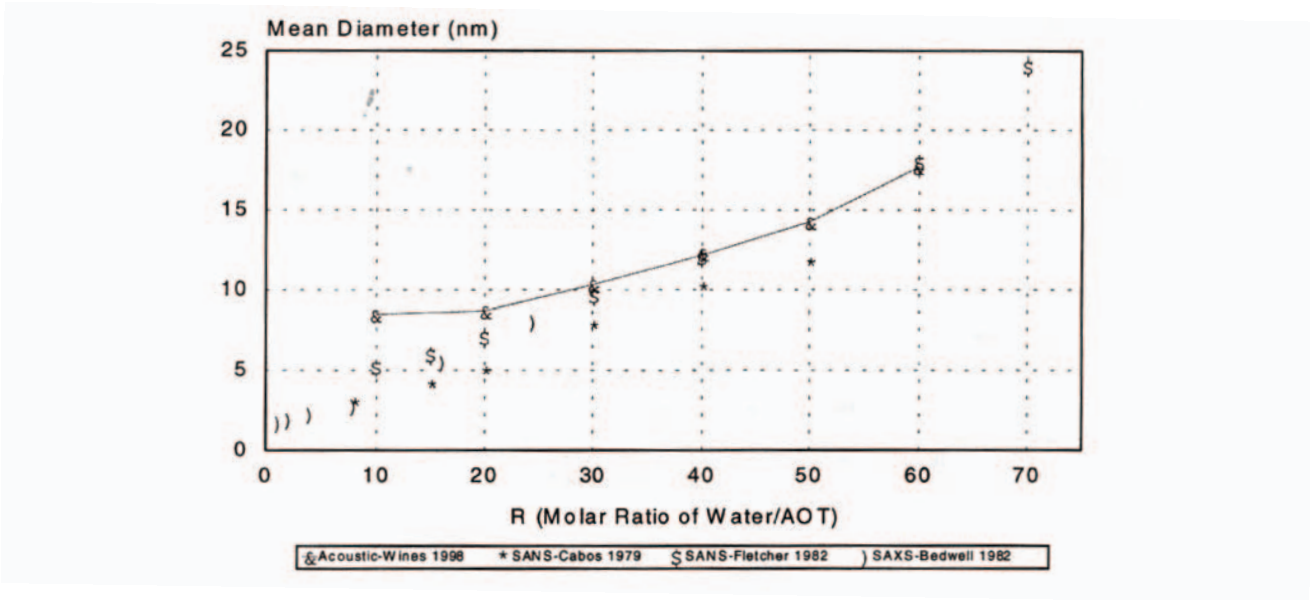

Figure 16 Comparison of mean droplet size measured using acoustic spectroscopy, neutron scattering, and X-ray scattering.

The contribution of droplets to the attenuation spectrum then may become too low to be reliably distinguished from the background signal coming from heptane molecules and AOT micelles.

In addition to particle size, the CVC was also measured for calculating zeta potential. The results are presented in Fig. 17, and ζ was found to depend on the water content. An increased concentration of water resulted in higher zeta potentials. However, the water content was not the most important factor. This experiment was performed at two different AOT con centrations and the ratio of water to AOT (R) was discovered to be the key parameter. When ζ wasplotted versus the R values, the same curve was obtained for both AOT concentrations. This demonstrates that the zeta potential depends on the degree of the water surface coverage by AOT molecules.

This experiment allows us to suggest a mechanism for electric-charge formation on the surface of the water droplets in the oil phase. This is a field of great interest in modern emulsion science. According to our experiment, the zeta potential appears when there is a deficit of AOT molecules for complete coverage of the water droplets. As more elements of the water phase become exposed to the oil, higher values of ζ are measured. The water phase also contains a considerable concentration of sodium ions that originate from the AOT and serve as counterions to the negatively charged sulfosuccinate head groups. As a result of decreased surface coverage, the water droplets gain surface charge when they are in contact with oil. This surface charge can appear because of ion exchange between the water and oil phases caused by the difference in standard chemical potentials in each phase. Molecules of AOT do not create surface charge, but conversely screen the surface charge of the initial water droplets. At the same time these AOT molecules change the interfacial tension, creating conditions for a thermodynamically stable microemulsion. This is only a hypothesis so far and further investigation is required for confirmation.

C. Latex Systems

There have been many successful experiments that have characterized latex systems by using both acoustics and electroacoustics. For instance, Allegra and Hawley (10) measurd polystyrene latex. We measured Standard Dow latex which is also polystyrene in nature (see above). There is another successful application, this time with neoprene latex, which is described in Ref. 15.

This low-density latex dispersion (Neoprene Latex 735A) is designed by DuPont as a wet-end additive to fibrous slurries. The fraction of the latex in the initial dispersion is 42.8% by weight (37.3% by volume). The pH value at 25°C is 11.5. The physical properties of the neoprene (slow crystallizing polychloroprene homopolymer) have been measured in the DuPont laboratories many years ago.

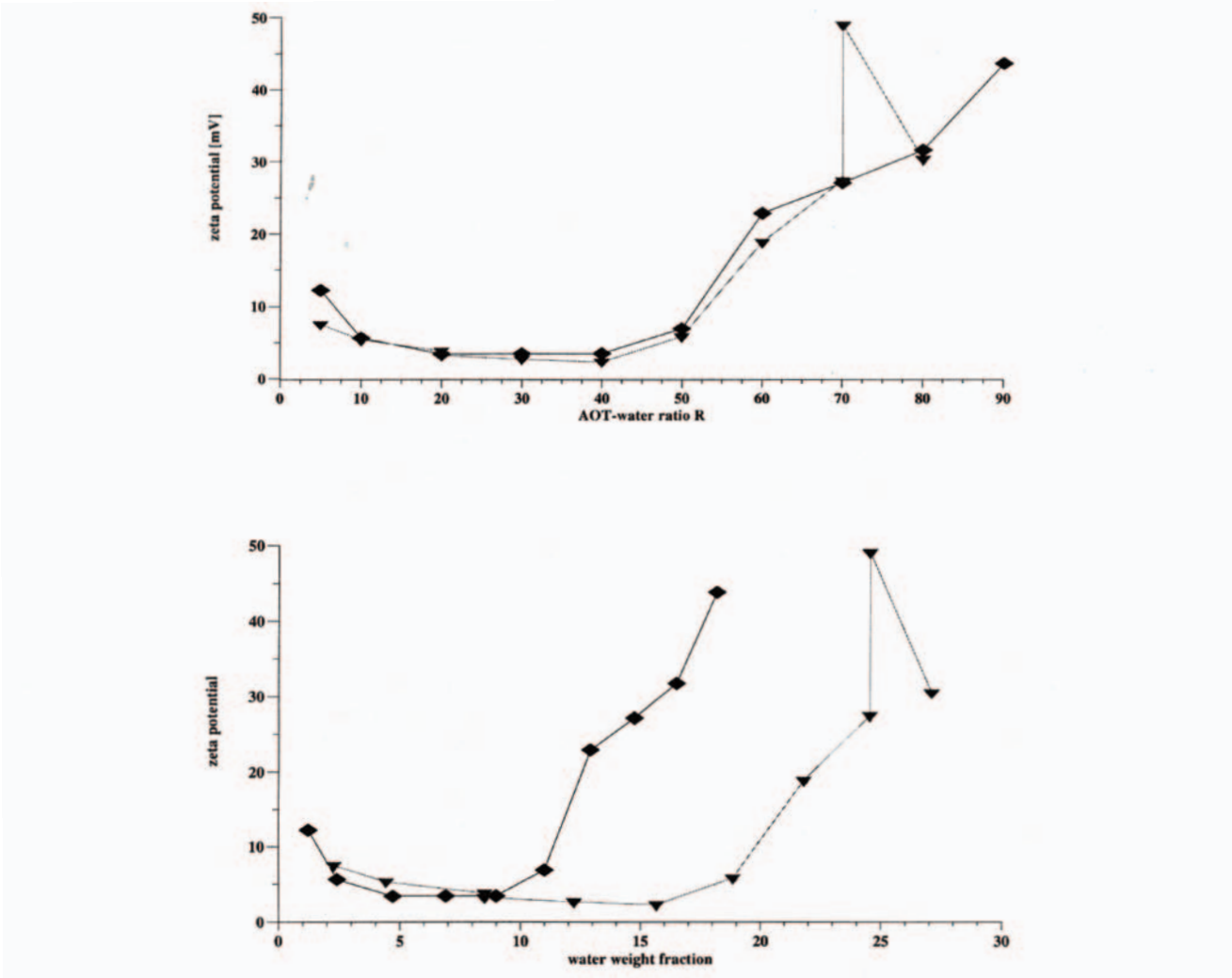

Figure 17 Zeta potential measured electroacoustically for water droplets covered with AOT in heptane vs. water content.

These data are summarized in the monograph "The Neoprenes" (62).

A dilution test was performed on this latex by using distilled water with a pH adjusted to 11.5 with 1 N potassium hydroxide. The samples were prepared with various dispersed concentrations (1.4, 4, 6.6, 13, 19.4, 25.6, 31.6, and 37.5 % by weight) by adding diluting solution to the initial neoprene latex.

Interpretation of the attenuation spectra requires information on the entire particle size spectra. A log-normal approximation was used with a median size of 0.16 μm and a standard deviation of 6% for the PSD measured with hydrodynamic chromatography.

The experimental data collected by the acoustic method with the neoprene latex provided an opportunity to check the validity of the ECAH theory when thermal losses were the dominant mechanism of the sound attenuation (see Fig. 18). In order to calculate the theoretical attenuation spectra, information is required about the particle size, thermodynamic properties of the dispersed phase, and dispersion medium materials as well as "partial intrinsic attenuations." Fortunately, all of the required parameters are available in this case. The approximate thermodynamic properties of the neoprene are known from the independent investigation performed by DuPont.

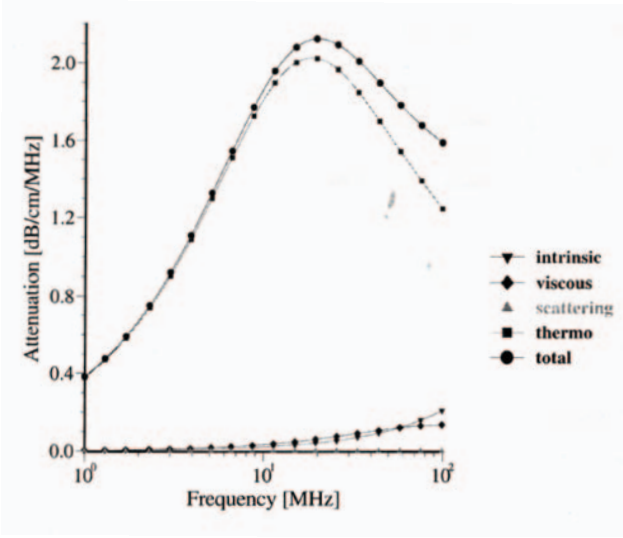

Figure 18 Theoretical attenuation spectra for the various mechanisms of the acoustic energy losses. Volume fraction is 10% vol; particle size 0.16 μm.

Figure 19 shows experimental and theoretical attenuation spectra for all the measured volume fractions. It is seen that the correlation between theory and experiment is very good up to 37.5% by weight (32.4% by volume).

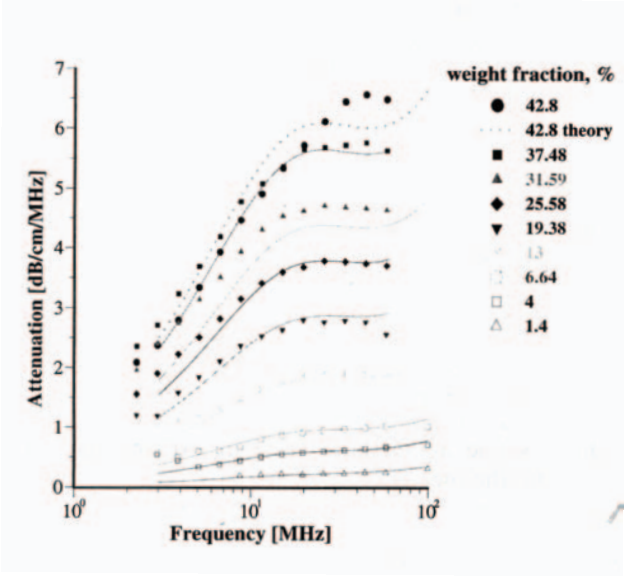

Figure 19 Experimental and theoretical attenuation spectra for neoprene latex for the weight fractions indicated in the legends.

These successful examples of characterizing latex systems are possible only when thermal expansion coefficients are known. Unfortunately, this parameter is not known for many latex polymers. This problem becomes even more complicated for latex systems than for emulsions because the value of the thermal expansion depends strongly on the chemical composition of the polymer. Figure 20 illustrates this fact for several ethylene copolymers with different ethylene contents. Variation of the ethylene content from 5 to 10% was found to cause significant change in the attenuation spectra. This change is associated with the thermal expansion coefficient, but not the particle size.

The uncertainty related to the thermal expansion coefficient makes latex systems the most complicated systems for acoustics. This is important to keep in mind for testing a particular model of an acoustic instrument. Latex dispersions that are used as standards for light-based methods should be used with caution as in many cases the thermal-expansion properties of these standards are not well known.

VIII. CONCLUSIONS

We hope that we have proved with this short review that acoustics and electroacoustics can be extremely helpful in characterizing particle size, zeta potential, and some other properties of concentrated emulsions, microemulsions, and latex systems. Both methods are commercially available already. There are still some problems with the theoretical background for electro-acoustics, but analysis of the literature shows gradual improvement in this field.

The combination of acoustic and electroacoustic spectroscopy provides a much more reliable and complete characterization of the disperse system than either one of those techniques separately. Electroacoustic phenomena are more complicated to interpret than acoustic phenomena because an additional field (electric) is involved. This problem becomes even more pronounced for a concentrated system. It makes acoustics favorable for characterizing particle size, whereas electroacoustics yields electric surface properties.

We believe that these ultrasound-based techniques provide a very valuable addition to the traditional colloid chemical arsenal of tools designed for characterizing surface phenomena.

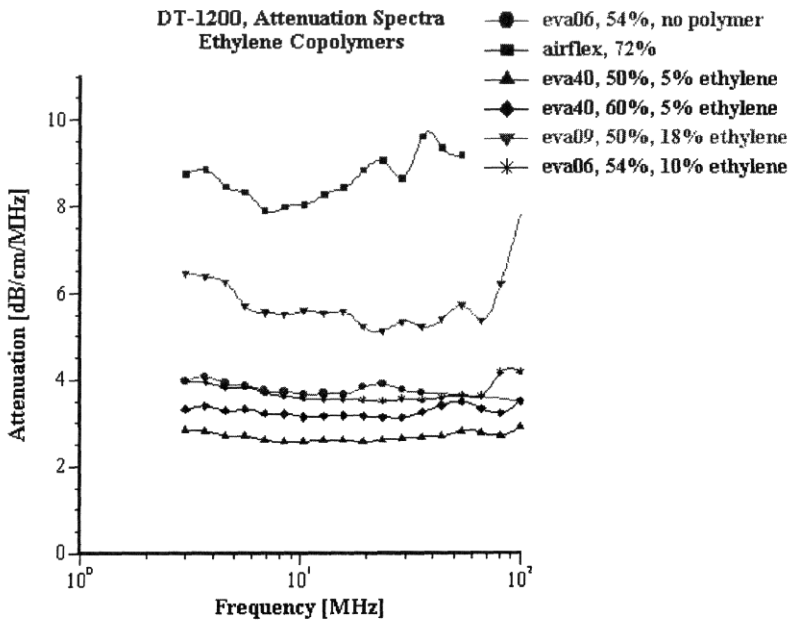

Figure 20 Attenuation spectra for latex dispersions with different contents of ethylene.

REFERENCES

1. JR Pellam, JK Galt. J Chem Phys 14: 608—613 (1946).
2. CTJ Sewell. Phil Trans Roy Soc, London, 210: 239—270, 1910.
3. PS Epstein, RR Carhart. J Acoust Soc Am 25: 553—565, 1953.
4. DJ McClements. Adv Colloid Interface Sci 37: 33—72, 1991.
5. VA Hackley, J Texter, eds. Ultrasonic and Dielectric Characterization Techniques for Suspended Particulates. New York: The American Chemical Society, 1998.
6. J Lyklema. Fundamentals of Interface and Colloid Science. Vol 1. New York: Academic Press, 1993.
7. RJ Hunter. Foundations of Colloid Science. Oxford: Oxford University Press, 1989.
8. RJ Hunter. Colloids Surfaces 141: 37—65, 1998.
9. TA Strout. Attenuation of Sound in High Concentration Suspensions: Development and Application of an Oscillatory Cell Model. Thesis. The University of Maine, 1991.
10. JR Allegra, SA Hawley. J Acoust Soc Am 51: 1545—1564, 1972.
11. JD McClements. Colloids Surfaces 90; 25—35, 1994.
12. DJ McClements. J Acoust Soc Am 91: 849—854, 1992.
13. AK Homes, RE Challis, DJ Wedlock. J Colloid Interface Sci 156: 261—269, 1993.
14. AK Holmes, RE Challis, DJ Wedlock. J Colloid and Interface Sci 168: 339—348, 1994. 15. AS Dukhin, PJ Goetz, CW Hamlet. Langmuir 12: 4998—5004, 1996.
16. LW Anson, RC Chivers. Ultrasonic 28: 16—25, 1990.
17. AH Harker, JAG Temple. J Phys D Appl Phys 21: 1576—1588, 1988.
18. RL Gibson, MN Toksoz. J Acoust Soc Am 85: 1925—1934, 1989.
19. AS Dukhin, PJ Goetz. Langmuir 12: 4987—4997, 1996.
20. U Riebel, et al. Part Part Syst Charact: 135—143, 1989.
21. R Chanamai, JN Coupland, DJ McClements. Colloids Surfaces 139: 241—250, 1998.
22. S Temkin. Phys Fluids 4: 2399—2409, 1992.
23. S Temkin. J Acoust Soc Am 103: 838—849, 1998.
24. RW O'Brien. J Fluid Mech 190: 71—86, 1988.
25. RW O'Brien. Determination of particle Size and Electric Charge. US Patent 5 059 909, 1991.
26. AS Dukhin, VN Shilov, Yu Borkovskaya. Langmuir 15 (10): 3452—3457, 1999.
27. AS Dukhin, H Ohshima, VN Shilov, PJ Goetz. Langmuir 15 (10): 3445—3451, 1999.
28. AS Dukhin, VN Shilov, H Ohshima. Langmuir 15 (20): 6692—6706, 1999.
29. LL Foldy. Propagation of Sound Through a Liquid Containing Bubbles. OSRD Report No. 6.1-sr 1130—1378, 1944.

30. EL Carnstein, LL Foldy. J Acoust Soc Am 19: 481—499, 1947.
31. FE Fox, SR Curley, GS Larson. J Soc Am 27: 534—539, 1957.
32. S Ljunggren, JC Eriksson. Colloids Surfaces 129/130: 151—155, 1997.
33. W Schaaffs. In: K Hellwege, ed. Molecular acoustics. Vol 5. Atomic and Molecular Physics. Berlin, New York: Landolt-Bornstein, 1967.
34. PS Waterman, RJ Truell. Math Phys 2: 512, 1961.
35. RR Irani, CF Callis. Particle Size: Measurement, Interpretation and Application. New York, London: John Wiley, 1971.
36. AS Dukhin, PJ Goetz. Colloids Surfaces 144: 49—58, 1998.
37. E Dickinson, DJ McClements, MJW Povey. J Colloid Interface Sci 142: 103—110, 1991.
38. JP Wilcoxon, RL Williamson. In: CR Safinya, SA Safran, PA Pincus, eds. Material Research Society Symposium Proceedings, Macromolecular liquids. Vol 177, Pittsburgh, PA: Materials Research Society, 1990.
39. F Candau. In: CR Safinya, SA Safran, PA Pincus, eds. Material Research Society Symposium Proceedings: Macromolecular Liquids. Vol 177. Pittsburgh, PA: Materials Research Society, 1990.
40. L Motte, A Lebrun, MP Pileni. Progr Colloids Polym Sci 89: 99, 1992.
41. D Ichinohe, T Arai, H Kise. Synth Metals 84: 75, 1997.
42. KV Schubert, KM Lusvardi, EW Kaler. Colloids Polym Sci 274: 875, 1996.
43. FM Menger, K Yamada. J Am Chem Soc 101: 6731, 1979.
44. D Chatenay, W Urbach, AM Cazabat, M Vacher, M Waks. Biophys J 48: 893, 1985.
45. GS Timmins, MJ Davies, BC Gilbert, H Caldarau. J Chem Soc Faraday Trans 90: 2643, 1994.
46. AV Kabanov. Makromol Chem, Macrormol Symp. 44: 253, 1991.
47. V Crupi, G Maisano, D Majolino, R Ponterio, V Villari, E Caponetti. J Mol Struct 383: 171, 1996.
48. B Bedwell, E Gulari. In: KL Mittal, ed. Solution Behavior of Surfactants. Vol 2. New York: Plenum Press, 1982.
49. E Gulari, B Bedwell, S Alkhafaji. J Colloid Interface Sci 77: 202, 1980.
50. M Zulauf, HF Eicke. J Phys Chem 83: 480, 1979.
51. HF Eicke. In: ID Rob, ed. Microemulsions. New York: Plenum Press, 1982, p 10.
52. JD Nicholson, JV Doherty, JHR Clark. In: ID Rob, ed. Microemulsions. New York: Plenum Press, 1982, p 33.
53. HF Eicke, J Rehak. Helv Chim Acta 59: 2883, 1976.
54. PDI Fletcher, BH Robinson, F Bermejo-Barrera, DG Oakenfull, JC Dore, DC Steytler. In: ID Rob, ed. Microemulsions. New York: Plenum Press, 1982, p 221.
55. PC Cabos, P Delord, J App Cryst. 12: 502, 1979.
56. S Radiman, LE Fountain, C Toprakcioglu, A de Vallera, P Chieux. Progr. Colloids Polym Sci 81: 54, 1990.
57. JP Huruguen, T Zemb, MP Pileni. progr Colloids Polym Sci 89: 39, 1992.
58. MP Pileni, T Zemb, C Petit. Chem Phys Lett 118: 414, 1985.
59. W Sager, W Sun, HF Eicke. Progr Colloids Polym Sci 89: 284, 1992.
60. SA Safran, GS Grest, ALR Bug. In: HL Rosano, M Clause, eds. Microemulsion Systems. New York: Marcel Dekker, 1987, p 235.
61. TH Wines, AS Dukhin, P Somasundaran. Colloids Surfaces, 2000.
62. NL Catton. The Neoprenes. Monograph. Rubber Chemical Division, EI Du Pont De Nemours, Wilmington, DE, 1953.